ANALYSIS OF CARBON-OXYGEN REACTION BY USE OF A SQUARE-INPUT RESPONSE TECHNIQUE AND ^{18}O ISOTOPE

Kouichi Miura and Hiroyuki Nakagawa
Department of Chemical Engineering, Kyoto University
Kyoto 606, Japan

Keywords: Gasification of carbon, Step response, ^{18}O isotope

INTRODUCTION

Carbon gasification reaction has been investigated for decades including the pioneering works of Walker and his co-workers[1], but its mechanism has not been completely elucidated. The concept of the active surface area (ASA) was proposed by them, and its importance has been recognized. However, since ASA was measured by O_2 chemisorption at below 300 °C where carbon loss through gasification is negligible, it does not reflect the actual gasification situation. To overcome this weak point, measurements of ASA in a batch reactor[2-4] and the so-called transient kinetic (TK) method were proposed[5,6]. Ahmed and Back[4] successfully measured the chemisorbed oxygen during the gasification using a batch reactor, and proposed a new mechanistic sequence for carbon-oxygen reaction which stresses the importance of the reaction between the gaseous oxygen and the chemisorbed oxygen. Radovic et al.[7,8] proposed the concept of the reactive surface area (RSA), and reported excellent proportionality between the CO_2 gasification rate and the RSA estimated by the TK and the TPD methods. Kapteijn et al.[9,10] showed that the TK method with labeled molecules is more powerful to examine the mechanism. They found the presence of two types of surface oxygen complexes which desorb at different rates.

Although the TK method is powerful, the method can trace only the desorption phenomena after a step change from an oxidizing gas stream to an inert gas stream. On the other hand, the step response technique changing an isotope stream to another isotope stream step-wisely enables us to observe *in situ* transient behavior without disturbing the reaction system if we can trace the change in all isotope species. This technique has been recently applied to carbon-oxygen reaction by Kyotani et al.[11]

The authors have recently proposed a Square-Input Response (SIR) method as a modification of the step response technique[12]. When we apply the SIR technique to carbon-oxygen reaction, we change the reactant stream containing $^{16}O_2$ step-wisely to the $^{18}O_2$ containing stream at a certain instant, and after a predetermined time interval we change the $^{18}O_2$ stream backwardly to the $^{16}O_2$ stream. This method enables us to observe transient changes on two step changes, to minimize the usage of expensive isotopes, and to facilitate the establishment of the balance of the isotope supplied as the square-input. We have successfully applied this technique to the analysis of a coal char gasification and to the analysis of the stabilization reaction of carbon fiber[13].

In this work the SRI technique was applied to the analysis of carbon-oxygen reaction to examine the reaction mechanism presented by the authors[14], and to determine the rate constants of elementary reactions.

EXPERIMENTAL

A mineral-free carbon black (CB) was used in this study. It was provided by Mitsubishi Chemicals and had the designation CB-30. The ultimate analysis of CB is C: 99.1%, H: 0.8%, and O: 0.1% on weight basis .
Figure 1 shows the apparatus used for the gasification experiments. About 3 to 12 mg of CB were embedded in a reactor made of quartz tube (4mm in ID and 30 cm in length). They were heated to 900 °C in a helium stream and held at this temperature for 10 minutes. Then they were cooled to a constant temperatures of 550, 570, or 600°C. To start the gasification, the helium stream was changed to the $^{16}O_2$ stream diluted by helium (22% conc.), whose flow rate was regulated by a mass flow controller at 50 ml/min. A part of the product gas was introduced to a pressure regulated section *via* a valve (V-2). The pressure of this section was kept at a few mmHg by regulating the opening of the valve V-2. Only a small amount of gas was introduced from this section to a mass spectrometer (MS; Nichiden Anerva, AGS211R), where signals for mass numbers of 28, 30, 32, 36, 44, 46, and 48 were continuously detected. To minimize the delay of the gas analysis from the gas formation, a small tubing (1/16 inch OD) was used and the gas flow in the pressure regulated section was designed as shown in the bottom of Fig. 1. The main flow exiting the reactor was led to a gaschromatograph (GC), where it was analyzed in every 10 minutes to determine precisely the concentrations of CO, O_2, and CO_2. By referring to these concentrations the signals of the MS were calibrated in every 10 minutes. Then the concentration of CO, O_2, and CO_2 in the product gas could be measured continuously and precisely.

The pure ^{18}O isotope (ISOTEC Inc.) containing 99.2 mol % ^{18}O was used for the SIR experiment. The isotope diluted by helium (22% $^{18}O_2$ conc.) was stored in a sample loop of about 50 ml as shown in Figure 1. When the conversion of CB reached 10 %, the 6-way

valve (V-1) was switched. Then the helium stream containing $^{16}O_2$ pushed out the $^{18}O_2$ containing gas in the sample loop to the reactor. The $^{18}O_2$ containing stream was supplied for about 1 min, and then the stream returned again to the stream containing only $^{16}O_2$. After the elapse of 20 min the temperature was raised to 900°C to combust the sample, and the ^{18}O retained in the sample was detected as $C^{18}O$, $C^{18}OO$, and $C^{18}O_2$. Using this technique, the exact ^{18}O balance could be established after changing the $^{18}O_2$ containing stream to the stream containing only $^{16}O_2$. The experiments using 1:1 mixture of $^{16}O_2$ and $^{18}O_2$ as the square-input were also performed to examine probable isotope exchange reactions. The experiments using pure He as the square-input were also performed. The experiments are performed to compare our results with those obtained by the so called TK experiments.

RESULTS AND DISCUSSION

Figures 2a and 2b show typical SIR results, where the formation rates of CO(28), CO(30). CO_2(44), CO_2(46), and CO_2(48) and the flow rate of O_2(36) are shown against the reaction time. Hereinafter, the isotopes are represented by the molecular weights in the brackets following the molecular formula. Figures 2c and 3, respectively, show the results obtained using the square-inputs of the 1:1 mixture of $^{16}O_2$ and $^{18}O_2$ and the pure He under the same experimental conditions as those in Fig. 2b.

First, we consider CO formation in Figs. 2a and 2b. On the step change from the $^{16}O_2$ stream to the $^{18}O_2$ (abbreviated to the $^{16}O_2/^{18}O_2$-step) the CO(28) formation rate decreased rapidly to a half or so, and then decreased gradually. The CO(30) formation rate responded almost instantaneously to the step change to increase a certain level, and increased gradually. On the step change from the $^{18}O_2$ stream to the $^{16}O_2$ (the $^{18}O_2/^{16}O_2$-step) almost reverse responses were observed. The CO(28) formation rate increased rapidly at first, then increased gradually. The CO(30) formation rate decreased instantaneously on the step change to a small value, then decreased gradually. These results clearly show that CO is formed at least two reactions. The gradual formation of CO(28) and CO(30) without the corresponding oxygen isotopes in the gas phase indicates that these are produced from the chemisorbed oxygen. The rapid changes of the formation rates of both CO(28) and CO(30) on the step changes are associated with the reaction between the gas phase oxygen and the active site.

The CO_2 formation rates are considered next. On the $^{16}O_2/^{18}O_2$-step the CO_2(44) formation rate responded almost similarly as the CO(28) formation rate. The CO_2(46) formation rate increased rapidly on the step change, but started to decrease gradually after reaching a maximum. The CO_2(48) formation rate responded slowly to the step change, but it increased monotonously. On the $^{18}O_2/^{16}O_2$-step the CO_2(44) formation rate again responded almost similarly as the CO(28) formation rate. The CO_2(46) formation rate decreased rapidly first, and then decreased gradually. The CO_2(48) formation rate decreased rapidly to a very small value, then decreased gradually. These results indicate that CO_2 is formed by several reaction paths: both the reaction between gaseous oxygen and chemisorbed oxygen and the reaction between chemisorbed oxygens are judged to be significant.

Both the total CO formation rate (the sum of the formation rates of CO(28) and CO(30)) and the total CO_2 formation rate (the sum of the formation rates of CO_2(44), CO_2(46), and CO_2(48))change little during the SRI experiments as shown in Figs. 2a to 2c. This indicates that the SIR experiment using ^{18}O is powerful to examine the reaction mechanism without disturbing the steady state of reaction as expected. This conclusion is further substantiated when comparing Figs. 2b and 3. The response behavior of CO(28) and CO_2(44) in Fig. 3, which is the TK experiment, is significantly different from that in Fig. 2b. The gradual formations of both CO(28) and CO_2(44) observed in Fig.2b were not observed in Fig. 3. This means that the rate parameters determined by the TK method is different from those under the gasification of steady state for at least this reaction system.

We presented the following gasification mechanism for carbon oxidation based on the pulse experiments using $^{18}O_2$ isotope[14].

$$2\,C_f + O_2 \rightarrow C(O) + CO \qquad [1]$$

$$2\,C_f + O_2 \rightarrow 2\,C(O) \qquad [2]$$

$$C(O) \rightarrow CO + C_f \quad (*) \qquad [3]$$

$$C_f + C(O) + O_2 \rightarrow C(O) + CO_2 + C_f \qquad [4]$$

$$C(O) + C(O) \rightarrow CO_2 + C_f \quad (*) \qquad [5]$$

$$C(O) + C(O) \rightarrow C(O) + C(O) \qquad [6]$$

where C_f and C(O) represent the free active site and the chemisorbed oxygen, respectively. We assumed that these reactions proceed only when gaseous oxygen is present. The mechanism is close to that proposed by Ahmed et al.[4] One of the great differences is that we assume the amount of the short-lived oxygen is immeasurably small as Walker et al. assumed in the earlier paper[3]. In other words, we assumed that the short-lived oxygen is formed through Eqs. 1, 2, 4 and 6 only when gaseous oxygen interacted with carbon surface and the oxygen complex. The reactions in which only the short-lived oxygen surface intermediate participates are marked by an asterisk (*).

The validity of the proposed mechanism can be examined in more detail using the results

obtained in this work. The balance of the ^{18}O after the $^{18}O_2/^{16}O_2$-step is easily established as stated above, because we analyzed all the ^{18}O containing species including the amount of ^{18}O retained in the sample. Then the amount of chemisorbed oxygen, $n_O(18)$, at a certain time is estimated by summing up the ^{18}O evolved as CO(30), CO_2(46), and CO_2(48) from the end of the reaction. Utilizing the $n_O(18)$ values estimated, the formation rates of CO(30) and CO_2(46)were plotted against $n_O(18)$ in Figures 4a and 4b at three reaction temperatures. Both rates increased with the increase of $n_O(18)$ as expected, but linear relationships did not hold. Since CO(30) is produced *via* Eq. 3, the CO(30) formation rate should be directly proportional to $n_O(18)$ if CO(30) was produced from only the stable oxygen complex. However, this was not the case, indicating that the contribution of the short-lived oxygen must be taken into account to explain the CO(30) formation. The relationship between the CO_2(46) formation rate and $n_O(18)$ in Fig. 4b cannot be explained by only Eqs. 4 and 5 as far as we assume only single oxygen complex.

Then the mechanism was rewritten assuming two active sites, C_A and C_B, and in consequence two oxygen complexes, $C_A(O)$ and $C_B(O)$, as follows:

$$C_A + O_2 \rightarrow C_A(O) + CO \quad ; r_{1A} \quad [7]$$
$$C_B + O_2 \rightarrow C_B(O) + CO \quad ; r_{1B} \quad [8]$$
$$2C_A + O_2 \rightarrow 2\,C_A(O) \quad ; r_{2A} \quad [9]$$
$$2C_B + O_2 \rightarrow 2\,C_B(O) \quad ; r_{2B} \quad [10]$$
$$C_A(O) \rightarrow CO + C_f \quad ; r_{3A} \quad [11]$$
$$C_B(O) \rightarrow CO + C_f \quad ; r_{3B} \quad [12]$$
$$C_A + C_A(O) + O_2 \rightarrow CO_2 + C_A(O) \quad ; r_{4A} \quad [13]$$
$$C_A + C_B(O) + O_2 \rightarrow CO_2 + C_A(O) \quad ; r_{4B} \quad [14]$$
$$C_B + C_A(O) + O_2 \rightarrow CO_2 + C_BO) \quad ; r_{4C} \quad [15]$$
$$C_B + C_B(O) + O_2 \rightarrow CO_2 + C_BO) \quad ; r_{4D} \quad [16]$$
$$C_A(O) + C_A(O) \rightarrow CO_2 \quad ; r_{5A} \quad [17]$$
$$C_A(O) + C_B(O) \rightarrow CO_2 \quad ; r_{5B} \quad [18]$$
$$C_B(O) + C_B(O) \rightarrow CO_2 \quad ; r_{5C} \quad [19]$$

where $C_A(O)$ and $C_B(O)$ represent the short-lived oxygen complex and the stable oxygen complex, respectively. The contribution of Eq. 6 was neglected, because the amounts of $C_A(O)$ and $C_B(O)$ do not change through the reaction. r_{1A} to r_{5C} represent the reaction rates.

The validity of the reaction mechanism was tested using the change in the ^{18}O containing species after the $^{18}O_2/^{16}O_2$-step. The mechanistic sequence for this case is simplified as follows:

$$C_A(^{18}O) \rightarrow C^{18}O \quad [20]$$
$$C_B(^{18}O) \rightarrow C^{18}O \quad [21]$$
$$C_A + C_A(^{18}O) + O_2 \rightarrow C^{18}OO + C_A(O) + C_f \quad [22]$$
$$C_A + C_B(^{18}O) + O_2 \rightarrow C^{18}OO + C_A(O) + C_f \quad [23]$$
$$C_A(^{18}O) + C_A(O) \rightarrow C^{18}OO + C_f \quad [24]$$
$$C_A(O) + C_B(^{18}O) \rightarrow C^{18}OO + C_f \quad [25]$$
$$C_B(^{18}O) + C_B(O) \rightarrow C^{18}OO + C_f \quad [26]$$
$$C_A(^{18}O) + C_A(^{18}O) \rightarrow C^{18}O_2 + C_f \quad [27]$$
$$C_A(^{18}O) + C_B(^{18}O) \rightarrow C^{18}O_2 + C_f \quad [28]$$
$$C_B(^{18}O) + C_B(^{18}O) \rightarrow C^{18}O_2 + C_f \quad [29]$$

Under the steady state gasification the total amount of chemisorbed oxygen, n_O, is kept constant, and both n_{OA} and n_{OB} would be kept constant. Then the following relationships would hold:

$$n_{OA} + n_{OB} = n_O \text{ (constant)} \quad [30]$$
$$n_{OA}(16) + n_{OA}(18) = n_{OA} \text{ (constant)} \quad [31]$$
$$n_{OB}(16) + n_{OB}(18) = n_{OB} \text{ (constant)} \quad [32]$$

Using the data for the changes in the ^{18}O species after the $^{18}O_2/^{16}O_2$-step and the relationships of Eqs. 30 to 32, we could determine the reaction rate constants, k_{3A}, k_{3B}, $k_{4A}[C_A]+k_{4B}[C_A]$, $k_{4C}[C_B]+k_{4D}[C_B]$, k_{5A}, k_{5B}, and k_{5C}, and the values of n_{OA}, n_{OB}, and n_O which appear in r_{3A}, r_{3B}, r_{4A}, r_{4B}, r_{4C}, r_{4D}, r_{5A}, r_{5B}, and r_{5C}. Then the rate constants, $k_{1A}+k_{1B}$, and $k_{2A}[C_A]+k_{2B}[C_B]$ could be estimated using the change in the formation rate of CO(28), the relationship of Eq. 30 and the parameters determined above. Thus all the rate constants were estimated, although some can not be determined independently. The rate constants at 570°C are shown in Table 2, and the calculated curves using these parameters are compared with the experimental data in Figure 5. Fairly good agreements were obtained between the calculated curves and the experimental data over the whole course of gasification, although most of the parameters were estimated using the changes in the ^{18}O species after the $^{18}O_2/^{16}O_2$-step. We could estimate the amounts of both n_{OA} and n_{OB}, and could clarify that n_{OA} is much smaller than n_{OB}. These results seem to support the validity of the mechanistic sequence given in Eqs. 7 to 19.

At 570°C the ratio of $r_{1A}+r_{1B} : r_{3A} : r_{3B}$ for the CO formation was 4 : 3 : 3, and the ratio of $r_{4A}+r_{4B} : r_{4C}+r_{4D} : r_{5A} : r_{5B} : r_{5C}$ for the CO_2 formation was 4 : 4 : 1 : 2 : 2. These values clearly indicate the importance of the direct reactions between the active site and the gaseous oxygen as well as the desorption and/or reaction of chemisorbed oxygen(s),

supporting the observations given in Figs. 2a to 2c.

CONCLUSION

A square-input response (SIR) technique was applied to analyze the carbon-oxygen reaction. Actual *in situ* transient behaviors of isotopes were successfully traced. Most significant findings are as follows: Existence of two oxygen complexes, one is short-lived and the other is rather stable, was clarified, and their amounts were estimated. The importance of the direct attack of the gaseous oxygen to the active site and/or the chemisorbed oxygen was clarified. In addition, the significant contributions of the desorption of the oxygen complex and the reaction between the complexes to the gasification reaction were notified. The TK method was found not to reflect *in situ* desorption behavior of the oxygen complex at least for the reaction system studied here. Relative importance of elementary reactions was clarified. Further investigation is under way to examine the soundness of the proposed reaction mechanism and the determined rate parameters.

Literatures Cited

1. Laine, N.R.; Vastola, F.J.; Walker, P.L., Jr. J.Phys.Chem. **1963**, 67, 2030- 2034.
2. Tucker, B.G.; Mulcahy, F.R. Trans. Faraday Soc. **1959**, 65, 274-286.
3. Vastola, F.J.; Hart, P.J.; Walker, P.L., Jr. Carbon **1965**, 2, 65-71.
4. Ahmed, S.; Back, M.H.; Roscoe, J.M. ACS Division Fuel Chemistry, **1989**, 34, No.1, 63-70.
5. Freund, H.; Fuel, 1986, 65, 63-66.
6. Nozaki, T.; Adschiri, T.; Furusawa, T. Fuel Process. Techn. **1990**, 24, 277-283.
7. Jiang, H.; Radovic, L.R. ACS Division Fuel Chemistry, **1989**, 34, No.1, 79-86.
8. Lizzo, A.A.; Jiang, H.; Radovic, L.R. Carbon **1990**, 28, 7-19.
9. Kapteijn, F,; Meijer, R.; Moulijn, J.A. Energy & Fuels **1992**, 6, 494-497.
10. Kapteijn, F,; Meijer, R.; Moulijn, J.A.; Cazorla-Amoros, D. Carbon, 1994, 32, 1223-1231.
11. Zhuang, Q.; Kyotanim T.; Tomita, A. Energy & Fuels **1995**, 9, 630-634.
12. Miura, K.; Zha, H.; Hashimoto, K. *Proc. 30th Conf. Coal Sci., Tokyo, Jpan, Oct. 25-26,* **1993**, 63-66.
13. Miura, K.; Nakagawa, H,; Carbon Hashimoto, K. Carbon **1995**, 33, 275-282.
14. Crick, T.M.; Silveston, P.L.; Miura, K.; Hashimoto, K.; Energy & Fuels **1993**, 7, 1054-1061.

Table 1 The Rate Cnstants at 570 °C

$k_{1A}+k_{1B}$	1.58	$min^{-1}\cdot kg^{-1}\cdot atm^{-1}$
$k_{2A}[C_A]+k_{2B}[C_B]$	1.78	$min^{-1}\cdot kg^{-1}\cdot atm^{-1}$
k_{3A}	1.1	min^{-1}
k_{3B}	0.075	min^{-1}
$(k_{4A}+k_{4B})[C_A]$	4.5	$min^{-1}\cdot atm^{-1}$
$(k_{4C}+k_{4D})[C_B]$	0.35	$min^{-1}\cdot atn^{-1}$
k_{5A}	1.2	$kg\cdot mol^{-1}\cdot min^{-1}$
k_{5B}	0.078	$kg\cdot mol^{-1}\cdot min^{-1}$
k_{5C}	0.01	$kg\cdot mol^{-1}\cdot min^{-1}$

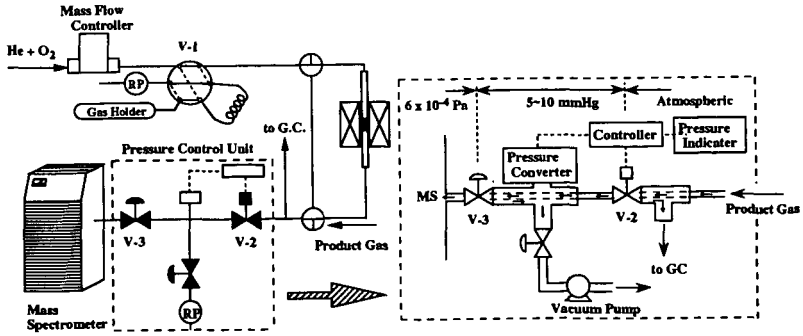

Figure 1 Experimental Apparatus

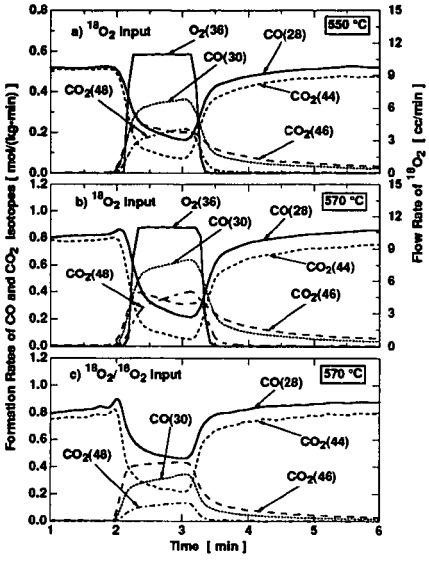

Figure 2 Changes in the formation rates of CO and CO_2 isotopes of the SIR experiment

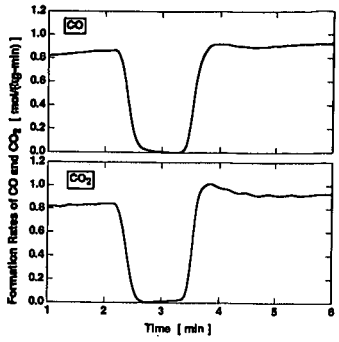

Figure 3 Changes in the formation rates of CO and CO_2 SIR experiment using square-input of the He (Equivalent to the TK technique)

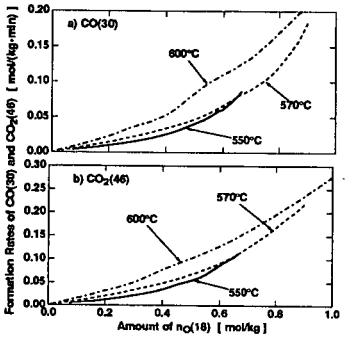

Figure 4 Relationships between formation rates of CO(30), CO_2(46) and n_O(18)

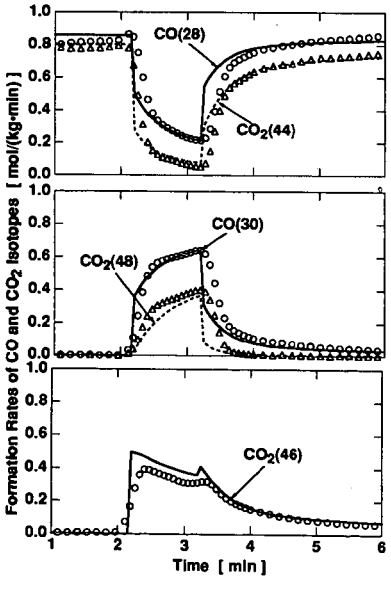

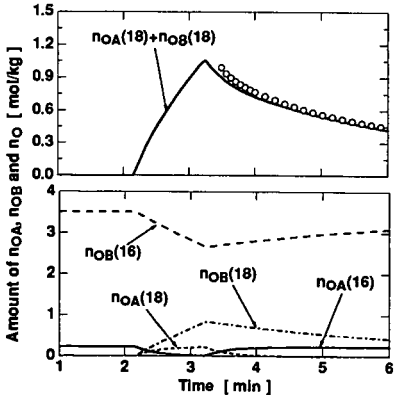

Figure 5 Comparison between the calculated curves and the experimental data (570°C, Lines:calculated, Keys:experimental data)